Towards a Real-Time Transduction and Classification of Chemoresistive Sensor Array Signals

Giovanni Pioggia, *Member, IEEE*, Marcello Ferro, and Fabio Di Francesco

***Abstract*—Recently, a growing interest in artificial implementations of biological systems has been arising. In particular, several research groups have been working in mimicking the mammalian olfactory system with the so-called electronic noses (e-noses). The e-noses, which are based on a sensor array, a fluid-dynamic system, and a data processing unit, are systems devoted to detecting and analyzing volatiles, where a deep knowledge of the target application is needed. In order to achieve effective results the sampling system, the measurement protocols, the sensor array, and the pattern recognition techniques have to be carefully designed. The increasing complexity of such design poses issues in sensory feature extraction and fusion, drift compensation, and data processing, especially when high efficiency is required for real-time applications. The interconnection and cooperation of several modules devoted to processing different tasks, such as control, data acquisition, data filtering interfaces, feature selection, and pattern analysis, are already mandatory. Moreover, heterogeneous techniques used to implement such tasks may introduce module interconnection and cooperation issues.**

In this paper, we address the development of a dedicated instrument able to perform real-time transduction, fusion, and processing of chemoresistive sensor array signals. In particular, this instrument realizes a dynamic and efficient management of data processing techniques and automatically controls the measurement protocols and the sampling system. An array of conducting poly (alkoxy-bithiophenes) sensors, the fluid-dynamic system, the electronic section, the framework's base architecture, and the implementation of dedicated application processes are described. The classification task is based on a self-organizing map where models for artificial neurons and connections were derived from the base structures available in the framework core. According to the target application, this instrument is portable and easily tailored, calibrated, and trained. Classification of olive oil headspaces supports its utility in supplying high-efficiency routine for volatile organic compounds detection and analysis.

***Index Terms*—Conducting polymer sensors, data processing, electronic nose, self-organizing maps, sensor array.**

I. Introduction

NOWADAYS e-nose technology is widespread [1]. An e-nose consists of a sampling system for volatiles, a partially specific chemical sensor array, an electronic apparatus able to control the sampling process and to collect the array transduction signals, and a pattern recognition algorithm trying to reproduce a human judgment or an analytic analysis of the sample. In the last decade, e-nose technology has been widely used to detect and analyze volatile organic compounds in the food industry [2]–[4]. Applications such as monitoring of emissions of outdoor [5] or indoor [6] volatile organic compounds, detection of explosives [7], and clinical diagnosis [8]–[10] are increasingly being considered. Materials such as phthalocyanines, metal oxides, and conducting polymers realize the sensor sensitive layer and allow a wide variety of chemical compounds to be detected [11]–[14]. Anyway the main sensor properties such as stability, repeatability, sensitivity, robustness, and lifetime are often a compromise in order to obtain a satisfactory reliability depending on the target application. Moreover, the increasing complexity of the e-nose architectures requires high-efficiency interconnection and co-operation of several heterogeneous modules, i.e., control, data acquisition, data filtering, feature selection, and pattern analysis [15]–[17]. Recently, a first step toward a standard design of multitransducer communication protocols and interfaces has been defined in IEEE 1451 [18], [19]. Enhancing the reliability of high-level processing systems represents the next critical step.

E-noses could answer to the need of a fast, simple, and objective analysis of volatiles. Experience has taught that great attention has to be paid, when dealing with e-noses, to avoiding inappropriate generalization of results that are only valid in a limited region of the experimental domain. In order to guarantee measurement accuracy, reliability, and repeatability, aside from the volatile nature, the sampling system must control and optimize all factors capable of influencing the generation of sensor transduction signals, while the electronic apparatus must be fast and accurate. It may not be simple to establish a multichannel communication among common artificial neural networks tools, feature extraction and selection processes, and acquisition and control systems [20], [21]. Moreover, high-level interfaces often do not allow adapting of the architecture and/or the process topology at run-time. As a result, complex processing methods have to be designed.

In this paper, we address the development of a high-efficiency fast and flexible instrument for real-time transduction, fusion, and processing of chemoresistive sensor array signals. The chemoresistive layers were synthesized via chemical polymerisation of poly (3, 3′-dipentoxy-2, 2′bithiophene) [14]. Doping reactions with four salts allowed differentiated resistance characteristics for an array of eight sensors. The chemico-physical interactions between sensing layers and volatile molecules result in an electric resistance variation for each sensor. The response of each sensor is thus an analog signal versus time

Manuscript received February 15, 2006; revised April 4, 2006. The associate editor coordinating the review of this paper and approving it for publication was Dr. Giorgio Sberveglieri.

G. Pioggia and M. Ferro are with the Interdepartmental Research Center E. Piaggio, Faculty of Engineering, University of Pisa, 56100 Italy (e-mail: giovanni.pioggia@ing.unipi.it; marcello.ferro@ing.unipi.it).

F. Di Francesco is with the Department of Chemistry and Industrial Chemistry, University of Pisa, 56100 Italy (e-mail: fdifra@dcci.unipi.it; ramsete@ifc.cnr.it).

Digital Object Identifier 10.1109/JSEN.2006.886893

which the electronic section acquires. Features such as raising time, steady-state, and peaks can be extracted processing the acquired signals. Features constitute the data set for the section devoted to the analysis and classification of volatiles. A preliminary investigation with reference products responsible for olive oil aromas was previously reported [24].

The instrument hardware can be divided into a hydraulic and an electronic section. The hydraulic section consists of a sampling system and an exposure chamber; the electronic section, developed taking into account the current techniques for noise reduction, consists of a central processing unit, a digital section, and an analog section. This system allows one to acquire reliable data from conducting polymer sensor arrays and to automatically control the sampling system and the experimental parameters. The software framework allows a dynamic and efficient management of heterogeneous data processing techniques. Synchronization among modules and data flow is managed by the framework. Specific control processes, pattern recognition algorithms, and sensor array interfaces were created inheriting from the framework base structures. The framework base architecture and the implementation of an application process based on a self-organizing map are described. In this paper, authors describe the detection and analysis of volatile compounds present in the headspace of olive oil samples.

II. Sensor Array

Chemoresistive conducting polymer sensing layers, which change their electrical conductivity in presence of volatiles, were deposited onto a substrate in correspondence of two or more metal electrodes. Conducting polymers may belong to conjugate or oligomer families polymerized by chemical or electrochemical techniques. A controlled doping with salts enables them to be conductive. This process complies with the development of a wide variety of sensors, whose response depends on the degree of affinity between volatile and the doped polymer. They work with temperatures lower than 60 °C; they are less sensitive than the metal oxide sensors and they suffer humidity. Fig. 1(a) reports the sensor layout and Fig. 1(b) the electrical equivalent circuit needed to measure the electric resistance of the sensing layer by means of the four probe method. The electric resistance (R_p) is calculated by dividing the voltage between the internal contacts (V_p) and the current injected between the external contacts (I_s). High-impedance measure of V_p allows the noisy contact resistances to be negligible. Sensor layout was realized depositing gold electrodes and contacts onto an $18 \times 12 \times 1$ mm^3 alumina substrate. Alumina permits a good adhesion of the polymeric film; it guarantees the electrical insulation and possesses a low degree of chemical reactivity. Contacts allow the sensing layer to be connected to the electronic apparatus.

The poly (3, 3′-dipentoxy-2, 2′bithiophenes)-based chemodetecting layers are prepared according to the procedure patented by De Rossi and Serra [22]. First, the monomers are chemically synthesized, polymerized, and neutralized. Neutralized polymers are thus doped with oxidizing salts such as cupric perchlorate, ferric perchlorate, cupric chloride, and iodine. The doping process consists of several steps. In a ratio of 100 mg/10 ml, the polymer is solved in a 1:1 volume ratio solution

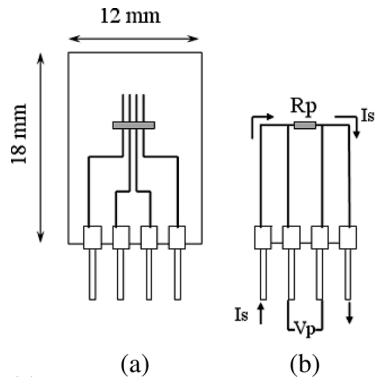

Fig. 1. Conductive polymer sensor (a) layout and (b) the electrical equivalent circuit.

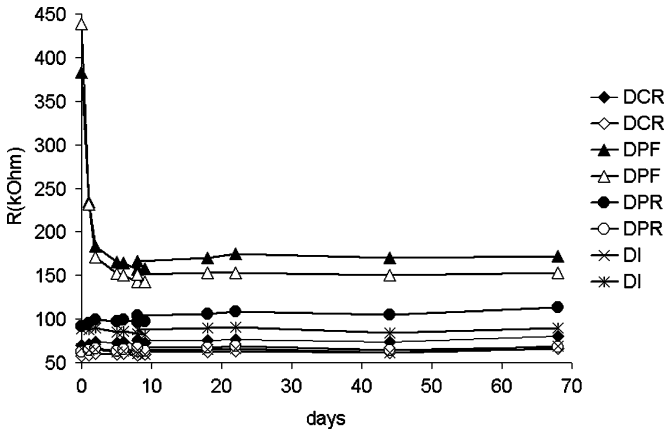

Fig. 2. Stability of doped poly (3, 3′-dipentoxy-2, 2′bithiophenes) sensors.

TABLE I
Doping Salts, Molar Ratios, Code, and Number of Selected Sensors

Doping salt	*M/Ox*	*Code*	*Number of sensors*
$CuCl_2$	3	DCR	2
$Fe(ClO_4)_3$	3	DPF	2
$Cu(ClO_4)_2$	3	DPR	2
I_2	3	DI	2

of trichloroethylene and chloroform. A solution obtained dissolving the doping salt in acetonitrile is added to the polymer suspension with the desired M/Ox (molar ratio). M represents the number of the monomeric units and Ox the number of doping molecules. In Fig. 2, the stability of eight doped poly (3, 3′-dipentoxy-2, 2′bithiophenes) sensors is reported. Doping salts, molar ratios, code, and number of sensors are summarized in Table I. Sensors can be produced with resistance variations in the range 500 Ω–1 MΩ. Characterization of responses of doped poly (alkoxy-bithiophenes) sensors exposed to organic vapours were previously reported from authors [14].

In order to deposit the polymeric sensing layer, a technique based on a three-axis micropositioning system was developed. The alumina support is placed onto the x–y axis, while a stainless steel microsyringe is placed onto the z axis. The deposition onto the alumina support is obtained in two steps. The poly (alkoxy-bithiophenes) suspension in chloroform or trichloroethylene is expelled from the needle of the microsyringe by means of an internal stainless steel wire; the substrate

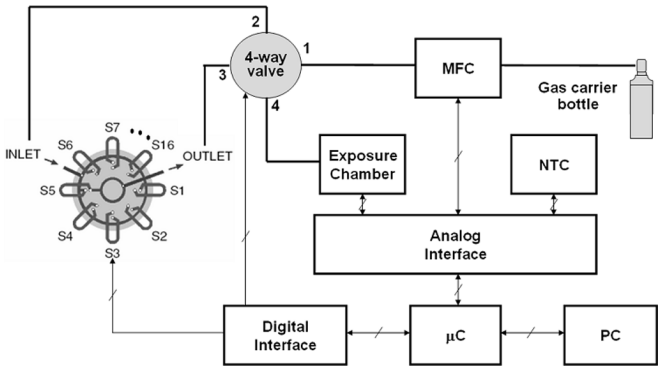

Fig. 3. Block scheme of the hardware section.

is simultaneously translated in order to realize the desired path. A stainless steel needle with an internal diameter of 110 μm was used. The relative motion of the three-axis micropositioning system, realized by three stepper motors, allows the geometry of the film to be controlled, avoiding a manual procedure. A stainless steel wire with a diameter of 80 μm can flow into the needle thanks to the z-axis stepper motor. The wire, kept in contact with the alumina substrate, helps to lay out the polymeric film. Moreover, the relative motion between the wire and the needle allows obstructions due to chloroform or trichloroethylene evaporation in correspondence of the needle tip to be avoided. This system allows sensing layers with lateral dimensions between 200 and 500 μm and grain diameters within 3 and 20 μm to be obtained.

III. Hardware Architecture

In this paper, we aim to realize a reliable and portable hardware architecture able to perform fast and accurate measurements with conductive polymer sensor array and to perform a dynamic and automatic control of the sampling process. Thus, in collaboration with Idronaut s.r.l., Milan, the electronic section was designed and realized taking into account the current techniques for noise reduction and for controlling each kind of sampling systems.

Fig. 3 shows a block scheme of the hardware architecture; it can be divided into a hydraulic section and an electronic section. In the hydraulic section, the sampling system conveys a volatile sample, by means of a gas carrier such as nitrogen or pure air, into an exposure chamber where sensors are lodged. The aim of the chamber is to expose in optimal conditions the sensor array to volatiles. The electronic section consists of a central processing unit, an analog interface, and a digital interface. The analog interface can drive up to 16 sensors with a resistance of the sensing layer within the range 500 Ω–1 MΩ. Shielded cables connect each sensor to the analog interface. For each sensor, a different current can be selected and injected thanks to 16 independent digital current generators. Each current generator is realized with a 12-bit digital-to-analog (D/A) converter, with a resolution of 1.22 μA per bit, which allows 4096 different currents to be chosen. The analog interface includes the electronics for controlling an array of mass flow controllers and the temperatures of two external devices. The acquisition of the sensor transduction signals is performed by 16 independent 24-bit delta–sigma differential analog-to-digital converters with a resolution of 298 nV per bit. The digital interface includes a 32-bit microcontroller, a 2 MByte nonvolatile memory for data, and a 1 MByte flash memory for system configuration. Moreover, it includes the electronics for driving and reading of external devices, in particular devoted to control a 16-way and a 4-way valve. It can work connected to the 220 V–50 Hz or to a rechargeable internal battery. In the standalone settings, it can be controlled by means of a liquid crystal display display and three function buttons; in the remote settings it can be controlled by means of an RS232 interface. The electronic section is included in a $27 \times 25 \times 7$ cm^3 box; its weight is 4 Kg.

A. Hydraulic Section

1) Sampling System: The instrument here proposed is devoted to the detection and analysis of volatile samples generated by the headspace of organic compounds. For this reason, the sampling system is composed of a bottle of ultrapure nitrogen, a mass flow controller (MFC), a four-way valve, and a 16-way valve connected to 16 125 ml glass vials containing 10 ml-solutions (2.5 μl/ml) of liquid samples. Inert PTFE tubing and fittings were used for the connections. A thermohygrometer inserted into one fitting allows humidity and temperature of the air flow to be measured. Vials were kept at a constant temperature of 25 °C within a metallic box. The 16-way valve allowed the selection of the sample to be analyzed, while the four-way valve was used to switch the system between state 1 (sensors flushed with nitrogen, baseline acquisition, and cleaning) and state 2 (exposure of sensors to odorant). The measurement protocol consists of three phases for each experiment:

- *baseline acquisition:* sensors flushed with nitrogen;
- *exposure:* sensors exposed to the sample headspace;
- *desorption and cleaning:* odors flushed away by nitrogen to restore baseline conditions.

2) Exposure Chamber: The sensor array can be housed in two eight-sensor stainless steel exposure chambers. Critical design points for an exposure chamber are as follows.

- *Sensor arrangement with reference to the incident flow:* an inadequate arrangement of sensors can lead to different exposure conditions among sensors.
- *Geometry:* sharp variations cause recirculating zones.
- *Dead volumes:* they extend the response time of the system and can cause uneven distribution of flow rate.

In order to expose an array of sensors to a chemical mixture in optimal conditions, the chamber must allow all the sensors to be simultaneously exposed under the same conditions, making it possible to accurately reproduce the shape of the input concentration signal at each sensor position. Moreover, it must be designed to obtain the same concentration profile in repeated measurements and short analyte concentration rise/fall times, to avoid memory effects and sample dilution. A homogeneous flow with low speed gradient, no recirculating zones or stagnant regions, and the same local concentration of volatiles over each sensor were obtained by choosing a radially symmetrical geometry for the chamber with a dedicated deflector, which allows homogeneous flow conditions with low velocity gradients [23].

B. Electronic Section

The electronics is lodged in a metallic shielded box to avoid outer electromagnetic interferences. It can also work as a stand-

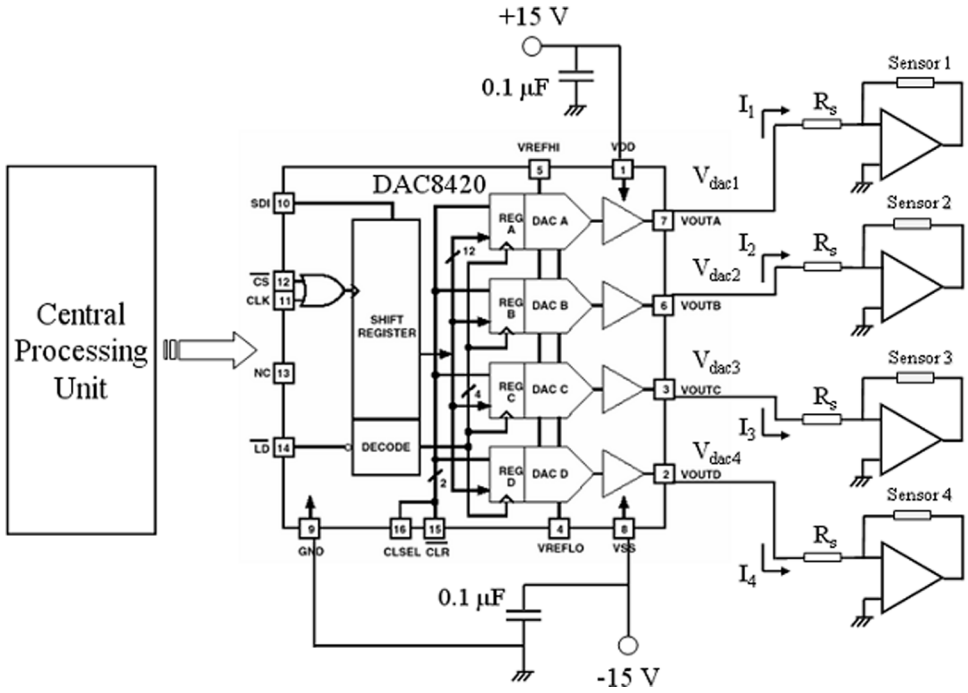

Fig. 4. Sensor driver for four sensors.

alone device, making use of an internal 12 V dc, 900 mA, 7 A/h rechargeable battery. It is provided with a 2 MB SRAM nonvolatile data memory and an RS232 serial interface for external programming and controlling. A central processing unit controls the whole device by means of an embedded 32-bit microcontroller MC68336 working at 20 MHz. The device allows the control of 16 independent user customizable polymer interfaces, each of them able to manage a conductive polymer sensor in the range of 500 Ω–1 MΩ by means of a polarization and preamplification circuitry. The device allows a scan rate of 0.1 s for 16 sensors to be obtained controlling in real-time the sampling system and the experimental protocols. A 1 MByte flash memory is used to store the management firmware and the system configuration. The protection of the stored data is performed through the extensive use of CRC-32 checking. The electronics possesses also four 0–5 V dc analog outputs with a resolution of 12 bit, 1.22 mV per bit.

1) Digital Interface: The digital section is mainly dedicated to the control of the sampling system. The central processing unit provides 12 open drain sink output ports. Each port allows a maximum load current of 100 mA and maximum working voltage 24 V dc. Two output ports are used to drive the four-way and 16-way valves. The other two output ports allow the control of the temperature of the sensor chamber and of the vials via two Proportional-Integral-Derivative (PID) controllers with an accuracy of 0.5 °C. The sensor chamber is provided with a PTC heater and an NTC thermistor, as well as the metallic box lodging the vials. Through one RS232 connector, a thermo-hygrometer interface and a dedicated communication protocol are implemented. The digital section also allows one to control, within the range 0 to 0.1 KHz, up to four stepper motors. The system includes a 2×40 character liquid crystal display and three buttons to interface the operator during the data acquisition operations performed without a personal computer connected.

2) The Sensor Driver: The sensor driver consists of controlled current generators, which produce different currents which aliment each sensor. Fig. 4 shows the block scheme for four sensors. It can drive up to 16 conducting polymer sensors. It contains 16 independent user customizable interfaces, composed by four D/A converters (DAC8420), 16 operational preamplifiers, and 16 scaling resistors (R_s).

The operational amplifiers are contained in four OP400 chips allowing a 10 MHz clock rate when ±15 V is supplied. The DAC8420 utilizes a unique compensate for different supply switch driver circuits in order to equally bias all DAC ladder switches and ensure an excellent linearity. The converter has a resolution of 2.44 mV or 1.22 μA, a settling time of 6 μs, and a maximum output voltage of 10 V, and it can drive up to 5 mA. More, it was chosen because it has a linearity that is monotonic over temperature and a low power consumption (35 mW max). The differential reference structure of the DAC8420 allows the user to determine both the upper and lower limits of the analog output voltage range avoiding unused regions. Thus the output range can be chosen between V_{refhi} and V_{reflo}. The V_{refhi} input of the DAC8420 will require both sourcing and sinking current capability from the reference voltage source. Many positive voltage references are intended as current sources only, and offer little sinking capability. They were set at +5 V and ground, respectively, with a current scaling resistor of 2 kΩ and a single +15 V supply. This allows one to drive a maximum current of 2.5 mA and to use conducting polymer sensors with intrinsic resistance ranging from 500 Ω to 1 MΩ.

The D/A forces an accurate voltage (V_{dac}) across the scaling resistor; thus the inverting amplifier forces a current of intensity V_{dac}/R_s through the sensor. The stability of the scaling resistor directly affects the current source temperature drift and stability. A 50 ppm/°C resistor (common for 1% metal film resistors) was used; thus the precision current source will

have approximately 50 ppm/°C drift with temperature. It is interesting to notice that the DAC8420 eliminated the need for external buffer amplifiers. The buffered outputs are simply short-circuit protected operational amplifiers connected as a voltage follower, and thus have output characteristics very similar to typical operational amplifiers. The output stage includes a p-channel metal–oxide–semiconductor (MOS) field-effect transistor to pull the output voltage down to the negative supply. It is very important in this single supply system; in fact V_{reflo} is connected to ground and thus the user can decide to remove a sensor in an experiment, cutting off the current flowing through the sensors. Like all amplifiers, the DAC8420 output buffers do generate voltage noise, 52 nV/Hz^{-1} typically, that was easily reduced by adding a simple RC low-pass filter on each output.

In order to ensure the accuracy performance, power supply and ground were carefully taken into consideration. The DAC8420 has a single ground pin that is internally connected to the digital section as the logic reference level. The digital ground is often noisy because of the switching currents of other digital circuitry. Any noise that is introduced at the ground pin could couple into the analog output. Thus, to avoid error causing digital noise in the sensitive analog circuitry, the ground pin was connected to the system analog ground. To reject the common-mode noise, the analog and digital ground was connected together at a single point in the system to provide a common reference. Moreover, each converter has two reference inputs and four analog outputs, which have moderate bandwidth and output currents. Thus in this circuitry, there is a significant potential for ground loops. To bypass this problem, the DAC8420 was connected to an ample supply filter, located as close as possible to the package. 0.1 μF ceramic capacitors provided a low impedance path to ground at high frequencies to handle transient currents due to internal logic switching. In order to preserve the specified analog performance of the device, the supply should be as noise-free as possible. Supply of 5 V for both the analog and digital circuitry was used. In order to avoid a noisy 5 V supply due to the fast edge rates of the popular complementary MOS logic families, as well as microcontroller or microprocessor which can have large current spikes during bus activity, a precision buried-zener-based voltage reference chip, that offers the best performance available from a single chip, was used.

3) MFC Driver: An MFC, which communicates by RS485 protocol, allows one to regulate the gas carrier flow rate in the range 0–500 ml/min. An RS485/RS232 interface allows the MFC to be driven. In order to control an array of MFCs, control connections coming from the array could be cabled on a unique RS485/RS232 data bus, allowing one to address and control the selected MFC.

4) NTC Interface: The temperatures of the vials and of the sensor chamber are digitally converted from two precalibrated NTC thermistors with dedicated preamplifiers. Two 10-bit analog-to-digital (A/D) converters with a resolution of 4.88 mV per bit were used. The measuring range results in 20–60°C with an accuracy of 0.5°C and a resolution of 0.1°C.

5) 24-bit Measuring System: Sensing devices, such as conducting polymer sensors, respond to physical and chemical occurrences that are measured and manipulated in the analysis and process control techniques. Sensing is a challenge where sensors used to detect small concentration of analytes and other environmental information produce low-level signals. In fact, these signals can easily be masked by ambient and electronic noise. The level of accuracy of an electronic nose can be improved increasing the signal-to-noise ratio (SNR). Several techniques, in the digital domain as well as in the analog domain, can be used to improve the SNR. The circuitry we adopted to improve the SNR for a sensor is shown in Fig. 5. In this circuit, thanks to its internal analog gain and its digital filtering capability, a delta–sigma A/D converter for each sensor was used. When it is properly configured, analog gain and digital filtering are optimized by the internal microcontroller to further improve the SNR.

The 24-bit measuring system contains 16 ADS1210 delta–sigma A/D converters. One converter for each sensor was used to increase the data conversion rate. The current flowing through the sensor generates a voltage that drives the A/D converter. The ADS1210 is a precision, wide dynamic range, self-calibrating single channel converter with 24-bit resolution (298 nV per bit) operating from a single +5 V supply. It contains a low-noise programmable gain amplifier (PGA), a second-order delta–sigma modulator, a programmable digital filter, a microcontroller including the instruction, command, and calibration registers, a serial interface, a clock generator circuit, and an internal 2.5 V reference. The ADS1210 was chosen to read differentially each sensor providing a good common-mode rejection over frequency. Moreover, it can be used in a single supply environment and can follow slowly moving signals. The differential inputs are especially suitable for direct connection to sensors or low-level voltage signals. In fact, the differential stage does not respond to common-mode input signals (common-mode rejection of 115 dB) and possesses an excellent power supply rejection. The output voltage is proportional to the equivalent resistance of the sensor. In particular, a positive digital output is produced if the analog input differential voltage is positive, while a negative digital output is produced whenever the differential voltage is negative. It is configured to convert differential voltage ranging from 2.5 to 2.5 V; this allows the use of sensors with intrinsic resistance ranging from 500 Ω to 1 MΩ.

In order to avoid a significant signal attenuation due to a direct connection of the sensor to the A/D converter, a buffer stage is used. The low-noise PGA, the A/D configuration, the timing generator, the dynamic range, and the sampling rate can be set by the user. In particular rates, modes and registers can be read or written via a synchronous serial interface. The data rate sets the number of samples that are used by the digital filter to obtain each conversion result. Each increase in the sampling rate produces a performance improvement for the same output data rate; trading off lower resolution results in higher data rates. A lower data rate results in higher resolution. It does not result in any appreciable change in power consumption. An onboard calibration circuit, which can work under request or automatically and continuously in background, allows internal offset and gain errors to be corrected.

IV. Software Architecture

A dedicated firmware allows the microcontroller to manage the electronic and the hydraulic sections. A communication protocol was designed to allow a personal computer to control the microcontroller tasks. A framework controls the synchroniza-

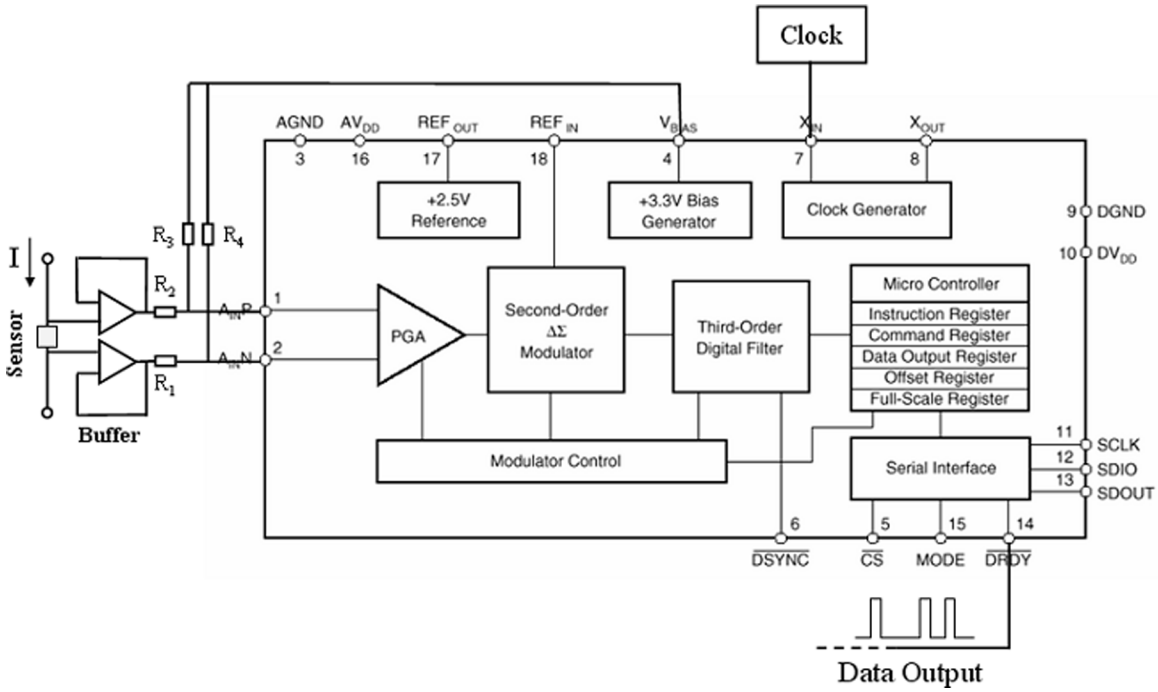

Fig. 5. Circuitry for differential acquisition of sensor signals.

tion of the data flow between the microcontroller and the personal computer through a framework I/O interface. The framework I/O interface has been developed in order to act as a buffer for the flow of information coming in and going out of the microcontroller.

The framework architecture has been designed as a hierarchical structure whose root is a manager module. It is realized as a high-level container of generic modules and represents the environment in which process modules and I/O filtering interfaces are placed. Modules may be grouped recursively in order to share common properties and functionalities of entity modules belonging to the same type. Communication channels are realized as connections through specific projection types that specify the connection topology. Connections are delegated to dispatch synchronization information and user-defined data. The filtering interface modules are able to drive the transducer hardware and to dispatch information to process modules. All base modules manage dynamic structures and are designed to maintain data consistency while the environment state may change. High-level processes such as control processes and pattern recognition algorithms are defined as application processes inside the framework. Such processes inherit properties and functionalities from the framework base structures, taking advantage of automation capabilities provided by the framework core. The framework allows setting up a communication language between the framework core and the hardware architecture. This guarantees an increased flexibility thanks to the presence of interfaces performing the function of interpreters for the specific hardware and filters which specify the way the framework core senses and communicates the information.

Several application processes run inside the framework core acting on data available into the framework I/O interface. The framework is able to control all the modules of the elaboration chain, including analysis protocol management and interfaces. During a signal preprocessing stage, various purposes are served, including baseline manipulation, compression, normalization, and drift compensation. Afterwards, data are sent to a dimensionality reduction module in order to perform a feature extraction. Selected features are ready for analysis, classification, and clustering tasks. A process devoted to data normalization gets sensory data from the framework I/O interface. Normalized data are sent to a process devoted to feature extraction in order to build the dataset. A Kohonen self-organizing map (KSOM) process performs the dataset classification task. A process devoted to the evaluation of the KSOM response shows the classification results. Communication channels are established as connections between application processes. Synchronization of processes and data flowing through connections is managed at run time by the framework. The presence of dynamic structures implies a configurable resource management, so the framework offers an optimized interface for enumeration and direct access requests. An inner synchronization signal is provided by the framework core to the processes and to the framework I/O interface, enabling one to gain time–space correlation.

V. Classification Process

In this paper, the classification task is performed by an application process based on a KSOM. Let $x_n^k(t)$ be the response of the nth of N sensors, i.e., the resistance of the sensor versus time t, to the kth of K samples. $x_n^k(t)$ signals were normalized over the exposure time, i.e., time interval $L = (t_1, t_2)$, resulting in function $\overline{x_n^k}(t) = x_n^k(t)/(x_{\min}^k - 1)$, where $x_{\min}^k$ represents the minimum value of $x_n^k(t)$ in the time interval L. We extracted from the normalized signals a set of F features; let $f_{n_1}^k, \ldots, f_{n_F}^k$ be the features. The features were the energy, i.e., $E_n^k = \sum_{i \in L} \overline{x_n^k}(t)^2$; the abscissa of the maximum value; the

angular coefficient of the line connecting $\overline{x_n^k}(t_1)$ and $\overline{x_n^k}(t_{\max})$; and the angular coefficient of the line connecting $\overline{x_n^k}(t_{\max})$ and $\overline{x_n^k}(t_2)$. Thus a dataset, where each response can be represented as a point in $\Re^{K\times F}$, was obtained. Features were normalized in the 0–1 interval.

In order to discriminate among samples of the dataset, a neural network approach was adopted [24]. A 3×3 KSOM [25] was applied. A KSOM maps the original space into a two-dimensional net of neurons in such a way that close neurons respond to similar signals. KSOMs are unsupervised neural networks, i.e., they exploit similarities of samples apart from the class which they belong to. In a KSOM, a *winner-takes-all* training algorithm is performed. For each input vector, the neuron that has the minimum distance $d = min_i\|\overline{f} - w_i\|$ from the input vector is the winning unit z. The weight w_{ij} of a generic neuron i at the time T for the input vector $\overline{f_n^k} = f_{n_1}^k, \ldots, f_{n_F}^k$ is modified as follows [26]:

$$w_{ij}(T) = w_{ij}(T-1) + \alpha(T) r_{iz}(T)\left[\overline{f}_j(T) - w_{ij}(T-1)\right]$$

where

$\alpha(T)$	$f_\alpha \alpha(T-1)$, learning rate with a learning rate factor;
$r_{iz}(T)$	$e^{-(d^2/\sigma^2)}$, feedback function of neuron i to the winning neuron z.
$\sigma(T)$	$f_\sigma \sigma(T-1)$, learning radius with learning radius factor f_σ.

The response of the KSOM is a nine-element Boolean vector; each element represents the activation function of a neuron. In order to check the generalization capability of the neural network, a cross-validation with three deletion groups was carried out. The data set was randomly partitioned in three equal-sized folds, i.e., 90 experiments for each fold. Two folds were held out for training, i.e., a 180 experiment training set, while the remaining fold, i.e., a 90 experiment test set, was used for testing. We fixed $\alpha(0) = 0.999$, $f_\alpha = 0.99$, $\sigma(0) = 5$, and $f_\sigma = 0.995$, and training epochs equal to 10 000.

VI. Experimental Results

This instrument has been used to analyze the headspace of certified olive oil samples. A trained panel test assessed 30 olive oil samples belonging to three equal-sized classes: extra virgin, virgin, and defected. Classes were denoted as $ExVg$, Vg, and Df, respectively.

Ten milliliters of each olive oil were sampled in three vials, for a total of 90 vials. Three series of measurements were performed for each vial at the same environmental conditions, for a total of 270 experiments. The KSOM learns to discriminate in such environmental conditions; therefore, in the case of uncontrolled environmental parameters, a new data set for each measurement campaign is needed. The experimental protocol consisted of 1200 samplings of baseline acquisition, 200 samplings of exposure, and 1400 samplings of desorption. Sensor responses were sampled with a scan rate of 0.1 s.

TABLE II
Mean and Standard Deviation Percentages of the Mean Confusion Matrix Resulting From the Three-Fold Cross-Validation

	ExVg		*Vg*		*Df*	
	mean	σ	*mean*	σ	*mean*	σ
ExVg	95.4	2.3	4.6	2.3	0.0	0.0
Vg	11.8	2.3	86.8	2.2	1.4	1.1
Df	0.0	0.0	3.9	1.9	96.1	1.9

A topological analysis of the KSOM showed for each test the presence of minimally overlapping zones. Labeling the three regions as belonging to $ExVg$, Vg, and Df classes allowed quantification of results obtained in the three-fold cross-validation. The performance of a classification system is commonly evaluated using the confusion matrix [27]. The generic element r_{ij} of the confusion matrix indicates how many times in percentage a pattern belonging to the class i was predicted as belonging to the class j. Table II summarizes the mean and standard deviation percentage values of the mean confusion matrix resulted from the three-fold cross-validation. It can be noticed that the extra virgin oils were never misclassified as defective and vice versa. A minimal misclassification can be observed for extra virgin and virgin. The accuracy rates for $ExVg$, Vg, and Df classes were, respectively, 95.4%, 86.8%, and 96.1%.

VII. Conclusions

In this paper, we have proposed and discussed a portable, reliable, and flexible instrument for transduction and processing of chemoresistive conducting polymer-based sensor array signals. The instrument is also able to automatically control the sampling system and the experimental parameters. The sampling system, the exposure chamber, and the measurement protocol were detailed. The electronic section was designed and realized taking into account the current techniques for noise reduction and for controlling each kind of sampling systems. In this paper, we detailed the instrument sections and the high-efficiency architecture for parallel management of data collecting, filtering, and processing. The interfaces with the sensor array and the actuators, the specific control and processing methods, and the data flowing through inner communication channels were described. We have also described the assessment of olive oil samples belonging to three classes: extra virgin, virgin, and defected. A total of 270 experiments were performed. A set of features was extracted in order to obtain a data set. To discriminate among data set patterns, a Kohonen self-organizing map was applied. We assessed the performance of our approach carrying out a three-fold cross-validation. A minimal misclassification was observed for extra virgin and virgin olive oils, while a null misclassification for defected olive as belonging to extra virgin oil was obtained. The accuracy rates were, respectively, 95.4%, 86.8%, and 96.1%.

References

[1] T. C. Pearce, S. S. Schiffman, H. T. Nagle, and J. W. Gardner, Eds., *Handbook of Machine Olfaction: Electronic Nose Technology*. Weinheim, Germany: Wiley-VCH, 2002.

[2] S. Ampuero and J. O. Bosset, "The electronic nose applied to dairy products: A review," *Sens. Actuators B, Chem.*, vol. 94, no. 1, pp. 1–12, 2003.
[3] T. Rajamäki, H.-L. Alakomi, T. Ritvanen, E. Skyttä, M. Smolander, and R. Ahvenainen, "Application of an electronic nose for quality assessment of modified atmosphere packaged poultry meat," *Food Contr.*, vol. 17, no. 1, pp. 5–13, 2006.
[4] D. L. Garcia-Gonzalez, N. Barie, M. Rapp, and R. Aparicio, "Analysis of virgin olive oil volatiles by a novel electronic nose based on a miniaturized SAW sensor array coupled with SPME enhanced headspace enrichment," *J Agric. Food Chem.*, vol. 52, no. 25, pp. 7475–7479, 2004.
[5] K. C. Persaud, P. Wareham, A. M. Pisanelli, and E. Scorsone, "Electronic nose—New condition monitoring devices for environmental applications," *Chem. Senses*, vol. 30, pp. 252–253, 2005.
[6] M. A. Ryan, H. Zhou, M. G. Buehler, K. S. Manatt, V. S. Mowrey, S. P. Jackson, A. K. Kisor, A. V. Shevade, and M. L. Homer, "Monitoring space shuttle air quality using the Jet Propulsion Laboratory electronic nose," *IEEE Sensors J.*, vol. 4, no. 3, pp. 337–347, 2004.
[7] J. Gardner and J. Yinon, Eds., *Electronic Noses and Sensors for the Detection of Explosives*. Berlin, Germany: Springer, 2004, NATO Science Series II: Mathematics, Physics and Chemistry.
[8] A. Logrieco, D. W. M. Arrigan, K. Brengel-Pesce, P. Siciliano, and I. Tothill, "DNA arrays, electronic noses and tongues, biosensors and receptors for rapid detection of toxigenic fungi and mycotoxins: A review," *Food Add. Contam.*, vol. 22, no. 4, pp. 335–344, 2005.
[9] R. F. Machado, D. Laskowski, O. Deffenderfer, T. Burch, S. Zheng, P. J. Mazzone, T. Mekhail, C. Jennings, J. K. Stoller, J. Pyle, J. Duncan, R. A. Dweik, and S. C. Erzurum, "Detection of lung cancer by sensor array analyses of exhaled breath," *Amer. J. Respir. Crit. Care Med.*, vol. 171, no. 11, pp. 1286–1291, 2005.
[10] M. E. Shykhon, D. W. Morgan, R. Dutta, E. L. Hines, and J. W. Gardner, "Clinical evaluation of the electronic nose in the diagnosis of ear, nose and throat infection: A preliminary study," *J Laryngol. Otol.*, vol. 118, no. 9, pp. 706–709, 2004.
[11] N. Pinna, G. Neri, M. Antonietti, and M. Niederberger, "Nonaqueous synthesis of nanocrystalline semi-conducting metal oxides for gas sensing," *Angewandte Chemie Int. Ed.*, vol. 43, no. 33, pp. 4345–4349, 2004.
[12] J. Brunet, A. Pauly, L. Mazet, J. P. Germain, M. Bouvet, and B. Malezieux, "Improvement in real time detection and selectivity of phthalocyanine gas sensors dedicated to oxidizing pollutants evaluation," *Thin Solid Films*, vol. 490, no. 1, pp. 28–35, 2005.
[13] K. Arshak, E. Moore, G. M. Lyons, J. Harris, and S. Clifford, "A review of gas sensors employed in electronic nose applications," *Sens. Rev.*, vol. 24, no. 2, pp. 181–198, 2004.
[14] M. C. Gallazzi, L. Tassoni, C. Bertarelli, G. Pioggia, F. DiFrancesco, and E. Montoneri, "Poly (alkoxy-bithiophenes) sensors for organic vapours," *Sens. Actuators B*, vol. 88, no. 2, pp. 178–189, 2003.
[15] A. N. Steinberg, "Data fusion system engineering," *IEEE Aerosp. Electron. Syst. Mag.*, vol. 16, no. 6, pp. 7–14, 2001.
[16] R. C. Luo, C.-C. Yih, and K. L. Su, "Multisensor fusion and integration: Approaches, applications, and future research directions," *IEEE Sensors J.*, vol. 2, no. 2, 2002.
[17] R. Gutierrez-Osuna, "Pattern analysis for machine olfaction: A review," *IEEE Sensors J.*, vol. 2, no. 3, 2002.
[18] K. Lee, "IEEE 1451: A standard in support of smart transducer networking," presented at the IEEE Instrum. Meas. Technol. Conf., Baltimore, MD, May 1–4, 2000.
[19] K. Lee and R. Schneeman, "Distributed measurement and control based on the IEEE 1451 smart transducer interface standards," *IEEE Trans. Instrum. Meas.*, vol. 49, no. 3, pp. 621–627, 2000.
[20] B. A. Snopok and I. V. Kruglenko, "Multisensor systems for chemical analysis: State-of-the-art in electronic nose technology and new trends in machine olfaction," *Thin Solid Films*, vol. 418, no. 1, pp. 21–41, 2002.
[21] J. Brunet, A. Pauly, L. Mazet, J. P. Germain, M. Bouvet, and B. Malezieux, "Improvement in real time detection and selectivity of phthalocyanine gas sensors dedicated to oxidizing pollutants evaluation," *Thin Solid Films*, vol. 490, no. 1, pp. 28–35, 2005.
[22] D. De Rossi and G. Serra, "Process for preparing electroconductive polymer films by doping with neutral polymers and chemical substances sensors obtained with these films," European Patent app. EP 99200904.3, 1999.
[23] F. Di Francesco, M. Falcitelli, L. Marano, and G. Pioggia, "A radially symmetric measurement chamber for electronic noses," *Sens. Actuators B*, vol. 105, no. 2, pp. 295–303, 2005.
[24] M. Chimenti, D. De Rossi, F. Di Francesco, C. Domenici, G. Pieri, G. Pioggia, and O. Salvetti, "A neural approach for improving the odour recognition capability of an electronic nose," *Meas. Sci. Technol.*, vol. 14, no. 6, pp. 815–821, 2003.
[25] T. Kohonen, *Self-Organising Maps*, 2nd ed. New York: Springer, 1997, vol. 30, Springer Series in Information Sciences.
[26] W. KinneBrock, *Neural Networks*. Munchen, Germany: Oldenburg Verlag, 1992.
[27] R. Kohavi and F. Provost, "Glossary of terms," *Machine Learn.*, vol. 30, pp. 271–274, 1998.

Giovanni Pioggia (M'05) was born in Messina, Italy, in 1972. He graduated in electronic engineering with a specialization in bioengineering from the University of Pisa, Italy, in 1997. He received the Ph.D. degree in biomimetic robotics from the University of Genova, Italy, in 2001.

Since 1998, he has been with the Interdepartmental Research Center "E. Piaggio," Faculty of Engineering, University of Pisa, where currently he is a Research Fellow of bioengineering and a contract Professor of models of biological systems. He collaborates with the Institute of Clinical Physiology, Italian Council of Research, and he is involved in several national and international projects. He was with the NASA Jet Propulsion Laboratory, Pasadena, CA, and also worked in Spain. His research activities concern biomedical systems, chemical sensors, design of sensors and actuators for bioengineering and robotics, signal processing, pattern recognition, artificial neural networks, and biomimetic robotics. He is author of more than 50 technical and scientific publications.

Marcello Ferro was born in Messina, Italy, in 1974. He graduated in electronic engineering with a specialization in informatics and microelectronics from the University of Rome La Sapienza, Italy, in 2001. He is currently pursuing the Ph.D. degree in automatics, bioengineering, and robotics at the Interdepartmental Research Center "E. Piaggio," University of Pisa, Italy, where he is involved in several international projects.

He collaborates with the Institute of Clinical Physiology, Italian Council of Research. His research activities are focused on artificial intelligence for biomimetic robotics, artificial neural networks, sensing and actuation interfaces, data analysis, and signal processing.

Fabio Di Francesco graduated as a physicist from the University of Pisa, Italy, in 1994.

He worked for two years on the development of mercury pollution detection methods with the Institute of Biophysics, Italian Council of Research (CNR). He then joined the Interdepartmental Research Center "E. Piaggio," where he started working on electronic noses with two distinct application areas, evaluation of olfactory annoyance of industrial emissions, and detection of olive oils defects. At present, he is a Research Scientist with the Institute of Clinical Physiology, CNR, where, within the MAST group, he is responsible for the development and use of electronic noses.